JACS
JOURNAL OF THE AMERICAN CHEMICAL SOCIETY
Communication
pubs.acs.org/JACS

Template Synthesis of Decaphyrin without *Meso*-Bridges: Cyclo[10]pyrrole

Tetsuo Okujima,*[,†] Chie Ando,[†] Saurabh Agrawal,[‡] Hiroki Matsumoto,[†] Shigeki Mori,[§] Keishi Ohara,[†] Ichiro Hisaki,[∥] Takahiro Nakae,[†] Masayoshi Takase,[†] Hidemitsu Uno,[†] and Nagao Kobayashi*[,‡]

[†]Graduate School of Science and Engineering, Ehime University, Matsuyama 790-8577, Japan
[‡]Faculty of Textile Science and Technology, Shinshu University, Ueda 386-8567, Japan
[§]Advanced Research Support Center, Ehime University, Matsuyama 790-8577, Japan
[∥]Graduate School of Engineering, Osaka University, Suita 565-0871, Japan

Supporting Information

ABSTRACT: An acenaphthylene-fused cyclo[10]pyrrole **1b** was selectively synthesized via an oxidative coupling reaction of the corresponding 2,2′-bipyrrole with the appropriate dianion template, croconate anion. The structure of **1b** as the isolated largest cyclo[*n*]pyrrole was elucidated by X-ray crystallographic analysis. The absorption spectrum exhibited a markedly red-shifted, intensified L band at 1982 nm, which was interpreted by application of Michl's perimeter and Gouterman's 4-orbital models, supported by magnetic circular dichroism (MCD) data and theoretical calculations.

In 2002, Sessler reported the first synthesis of cyclo[8]pyrrole, a ring-expanded porphyrin analogue with no *meso*-bridges.[1a] The photophysical, anion-binding, and liquid crystal properties of cyclo[*n*]pyrroles ($n = 6-8$) have been studied in-depth, along with their electronic structures.[1] Recently, some preparative examples of cyclo[8]pyrrole have been reported for derivatization at β-pyrrolic positions. For example, the introduction of fused aromatic-rings resulted in a dramatic shift of the absorption bands, and an intense band was observed at around 1000 nm.[2,3] However, little is known about larger structural analogues of cyclo[*n*]pyrroles ($n > 8$). Sessler, Kim, and Bucher have reported the electrochemical synthesis of a thiophene-containing cyclo[9]pyrrole, cyclo[3]thiophene[6]pyrrole, in 2012.[4] Sessler, Kim, and Ishida have also reported cyclo[6]pyridine[6]pyrrole synthesized by Suzuki–Miyaura cross-coupling in 2014.[5] These are hybrid macrocycles of cyclo[*n*]pyrrole. To our knowledge, there are no reports of the selective synthesis of larger analogues of cyclo[*n*]pyrrole ($n > 8$) composed only of pyrroles.

We report, herein, the synthesis of cyclo[10]pyrroles via an oxidative coupling reaction of the corresponding 2,2′-bipyrrole with the appropriate dianion template, croconate anion. The molecular structure was successfully elucidated by X-ray crystallographic analysis, while the optical properties and electronic structures have been analyzed using magnetic circular dichroism (MCD) spectroscopy and time-dependent (TD) DFT calculations.

Recently, we reported the synthesis of acenaphthylene-fused cyclo[8]pyrrole.[2b] Two conformational isomers of cyclo[8]-pyrrole were obtained as two red fractions with R_f values of 0.6 and 0.9 by column chromatography on silica gel with $CHCl_3$.[2b] In the TLC of the reaction mixture, a red spot was found with an R_f value of 0.0. The MALDI–TOF mass data of this fraction indicated the formation of trace amounts of larger structural analogues. After several fractions had been collected during the purification of the cyclo[8]pyrroles, a cyclo[10]-acenaphthopyrrole **1a** was isolated and purified by repeated column chromatography and GPC. The structure was confirmed by X-ray crystallographic analysis, which showed that alternating pyrrole moieties tilted above and below the mean plane, as shown in Figure S1.[6–9] Although the cyclo[10]pyrrole crystallized in a triclinic unit cell (space group $P\bar{1}$, $Z = 1$), it was not possible to determine the identity of the dianion bound in the inner cavity of the macrocycle. In the absence of a dianion, the π-system does not satisfy Hückel's rule for aromaticity since there would be 40 π-electrons on the inner perimeter.

Although cyclo[8]pyrroles were obtained in high yield by oxidative coupling of 2,2′-bipyrroles in the presence of H_2SO_4, the yields became low in the presence of HCl. Thus, the template effect of the SO_4^{2-} anion is important for building an octapyrrolic skeleton. Cylco[6]- and cyclo[7]pyrroles were generated by oxidative coupling with HCl, along with cyclo[8]pyrrole.[11] The yield of thiophene-containing cyclo[9]pyrrole was 6.5% by electrochemical synthesis, while the cyclo[9]pyrrole was not obtained by standard chemical oxidative coupling.[4] Although mass spectra indicated the formation of cyclo[5]-naphthobipyrrole and cyclo[10]naphthobipyrrole in the case of the synthesis of cyclo[4]naphthobipyrrole, these larger analogues were not isolated.[3a] Thus, an appropriate dianion template is necessary to synthesize larger analogues of cyclo[*n*]-pyrrole.

Initially, we attempted insertion of a dianion into the central cavity of **1a**. A solution of **1a** in $CHCl_3$ was mixed with aqueous $Na_2WO_4 \cdot 2H_2O$ to insert a larger dianion compared to SO_4^{2-}, and then stirred under acidic conditions (Scheme 1). The MALDI–TOF MS did not show a molecular ion peak of the tungstate salt (the WO_4^{2-} anion is too small to form hydrogen-bonding interactions with pyrrolic NHs). The central dianion must have a specific size to fit the cavity of cyclo[10]pyrrole and a pentagonal skeleton to form hydrogen-bonding with the 10

Received: May 13, 2016
Published: June 6, 2016

DOI: 10.1021/jacs.6b04941
J. Am. Chem. Soc. 2016, 138, 7540–7543

Scheme 1. Synthesis of Cyclo[10]pyrrole 1b (Croconate Salt of 1a)

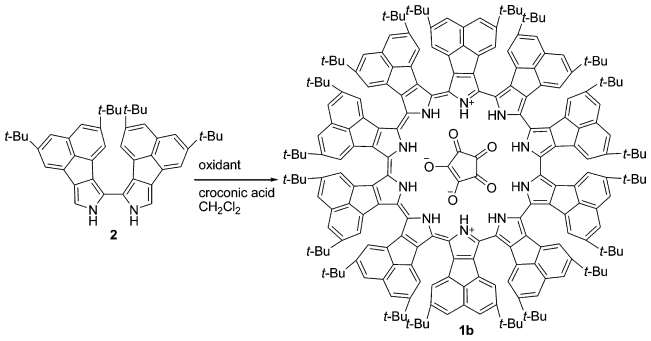

pyrrolic NHs, and in this respect, the croconate anion is expected to coordinate to this decapyrrolic macrocycle. After addition of aqueous croconic acid to a solution of **1a** in $CHCl_3$, the mixture was stirred for 3 days. In the TLC (silica, $CHCl_3$) of the reaction mixture, a red spot with an R_f value of 0.0 disappeared, and a new red spot with an R_f value of 1.0 was observed. This red fraction showed a molecular ion peak of the croconate salt of **1a** in the MALDI–TOF MS.

Oxidative coupling of 2,2′-bipyrrole **2** in CH_2Cl_2 was carried out in the presence of croconic acid. $FeCl_3$ and AgO were used as oxidants, to afford cyclo[10]pyrrole **1b** in 66 and 46% yields, respectively. Upon characterization by MS, NMR spectroscopy, and X-ray crystallographic analysis, the product was found to be consistent with the target structure of **1b**. The MALDI–TOF mass spectra showed two peaks assigned as M^+ and [M–croconate]$^+$. The ^{1}H NMR spectra of the products showed many signals for the acenaphthylene moieties in the aromatic region, and several signals for the NH protons between 5–7 ppm, similar to that of the asymmetrical conformer of cyclo[8]-acenaphthopyrrole.[2b] Although thermal isomerization to symmetrical **1b** was explored, the NMR spectra did not change after heating a solution of **1b** in *o*-dichlorobenzene at reflux. After removal of the croconate anion, thermal isomerization was carried out. When a solution of **1b** in CH_2Cl_2 was treated with 1 M NaOH, the color of the solution changed from red to yellow. After the yellow organic layer was separated and concentrated, a solution of the residue in toluene was refluxed for 4 days and treated with 0.01 M croconic acid. Recrystallization from CH_2Cl_2/*n*-hexane afforded a red solid, which did not show sufficient solubility to measure NMR. However, the MALDI–TOF MS and the absorption spectrum supported the structure of **1b**.

A single crystal of **1b** was obtained after recrystallization from chlorobenzene/*n*-heptane and was used for X-ray crystallographic analysis. The crystal structures are shown in Figure 1, with the crystallographic data summarized in Table S1. Compound **1b** crystallized in a triclinic unit cell (space group $P\bar{1}$, $Z = 2$). Alternating pyrrole moieties tilt above and below the mean plane, similar to **1a** (Figure S1). The inner croconate anion is bound by ten hydrogen-bonding interactions with NH···O distances of 1.784–2.015 Å, which are slightly shorter than the distances between the SO_4^{2-} anion and the pyrrolic NH of cyclo[8]pyrroles since the croconate anion adopts the planar structure.[1a,2,3] Thus, croconate anion acts as a template for cyclization because its size fits with the central space of the pyrrolic macrocycle. Dihedral angles of 14.1–18.0° and 30.4–32.9° are observed between the mean plane and pyrrole moieties and between adjacent pyrrole moieties, respectively, which are

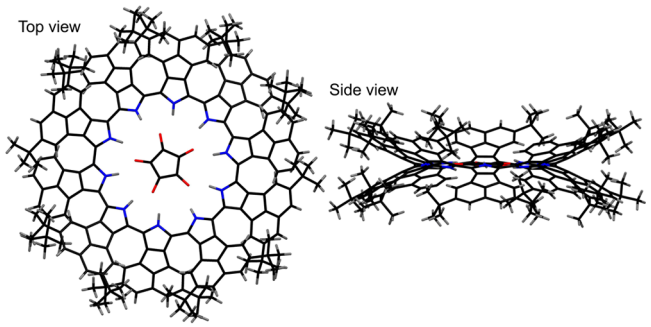

Figure 1. Molecular structure of cyclo[10]acenaphthopyrrole **1b**. Disordered (less popular) atoms and solvents are omitted for clarity.

similar to those of the symmetrical conformational isomer of cyclo[8]acenaphthopyrrole.[2b]

The electronic absorption and MCD spectra of **1b** are shown in Figure 2, together with its calculated absorption spectrum

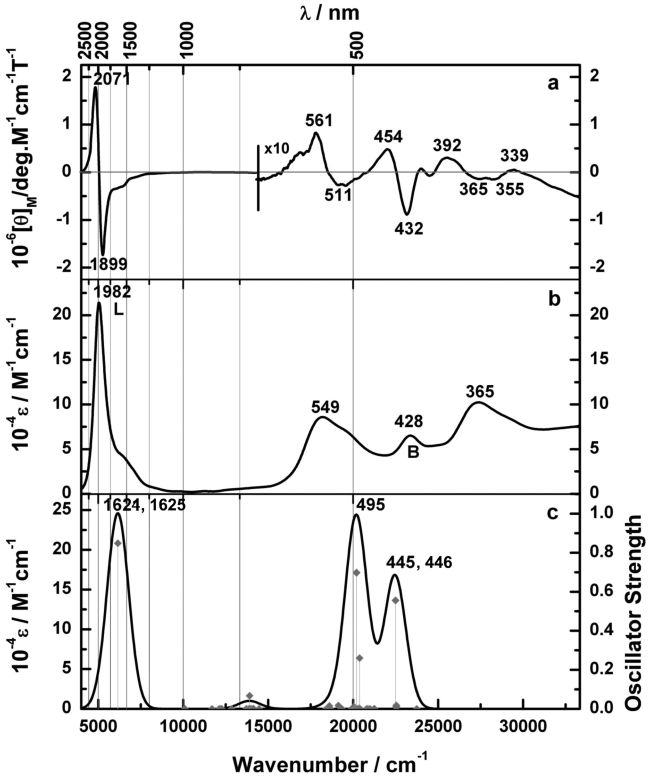

Figure 2. Experimental (a) MCD and (b) UV–vis–NIR and (c) calculated UV–vis–NIR spectra of cyclo[10]acenaphthopyrrole using the B3LYP/SDD level.

(Table S2).[10] The L band appeared at 1982 nm compared with 1481 nm for cyclo[8]acenaphthopyrrole.[2b] Thus, the expansion of two acenaphthopyrroles has resulted in markedly red-shift of the L band by ca. 500 nm (ca. 1710 cm^{-1}). In the UV–visible region, absorption peaks are observed at 549, 428, and 365 nm. In the MCD, negative $\mathcal{A}$-term-like curves were observed corresponding to most of the absorption peaks, with an apparent L band intensity about 20 times larger than that of the other bands.[12] From the sharp dispersion-type MCD curve and the results of molecular orbital calculations described later, the band at 428 nm appears to be the B band. These optical properties can be understood with reference to a $C_{30}H_{30}^{8-}$ parent hydrocarbon

DOI: 10.1021/jacs.6b04941
J. Am. Chem. Soc. 2016, 138, 7540–7543

that corresponds to the inner ligand perimeter with MOs arranged in an M_L = 0, ±1, ±2,... ±13, ±14, 15 sequence in ascending energy.[13] An allowed B band and a forbidden L band are related to $\Delta M_L = \pm 1$ (transitions from $M_L = -9$ to -10 and $M_L = +9$ to +10 MOs) and $\Delta M_L = \pm 19$ (transitions from $M_L = -9$ to +10 and $M_L = +9$ to -10 MOs) properties, respectively. Since the MCD intensity mechanism is based on the relative magnitude of the magnetic moments of the $\pi\pi^*$ excited states, the intensity of the L MCD band with "$\Delta M_L = \pm 19$" property is much (around 20 times) stronger than that of the B band with $\Delta M_L = \pm 1$, as is observed experimentally (Figure 2).

Figure 3 shows the MO energies and some MOs in TD-DFT calculations based on the B3LYP-optimized geometry of **1b**,

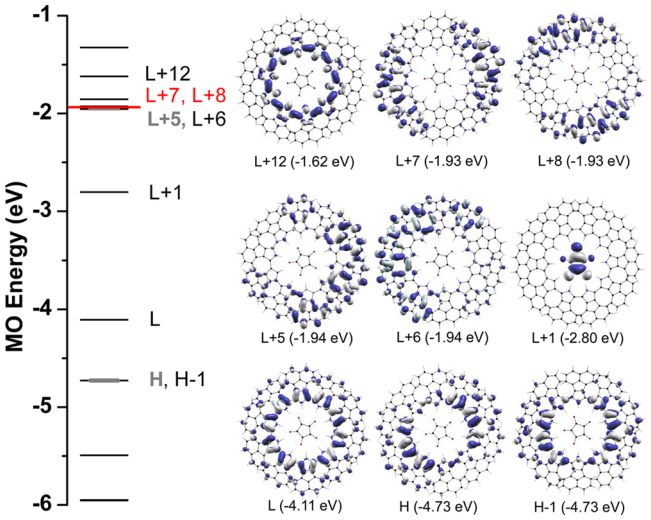

Figure 3. Partial molecular energy diagram and some orbitals contributing to absorption spectrum for the B3LYP-optimized geometries of **1b**. Note that L + 1 is not ligand-centered.

which is close to its X-ray structure (Table S1). In compound **1b**, some degenerate orbitals in a high-symmetry parent hydrocarbon perimeter are raised, due to a structural perturbation. When the C_{30} axis of $C_{30}H_{30}^{8-}$ is replaced by an S_5 in the proper rotation axis in the context of D_{5d} symmetry with respect to **1b**, only the degeneracy of MOs with M_L = odd number is retained, while that of those with M_L = even number are split. This outcome means that the HOMOs ($M_L = \pm 9$) are degenerate in **1b**, while the LUMOs ($M_L = \pm 10$) are split, in contrast to normal D_{4h} type porphyrinoids, in which the HOMOs with $M_L = \pm 4$ are symmetry-split, while the LUMOs with $M_L = \pm 5$ are degenerate.[14] In understanding the MCD spectra of chromophores, the degeneracy in the ground and/or excited states and the relative energy splitting of the HOMO and HOMO − 1 (ΔHOMO) and LUMO + 1 (in the present study LUMO + 12) and LUMO (ΔLUMO) are important. When the excited state is orbitally degenerate, as in this case, a derivative-shaped MCD curve (called $\mathcal{A}$-term) is observed, associated with an absorption peak, and its signal changes from plus-to-minus if ΔLUMO > ΔHOMO is in ascending energy.[13] Conversely, a minus-to-plus MCD pattern appears if ΔLUMO < ΔHOMO, as is generally seen for normal porphyrinoids. In accordance with these MCD characteristics, **1b** showed a plus-to-minus MCD sequence corresponding to both the L and B bands.

The calculated absorption spectrum in Figure 2c broadly reproduces the experimental data. The L and B bands were calculated at 1625 (and 1624) and 446 (and 445) nm, and from the configuration shown in Table S2, the band estimated at 495 nm corresponds to transitions from the HOMO − 1 to the fused acenaphthylene-centered orbitals (LUMO + 2 to LUMO + 11). The emergence of a red-shifted, intensified L band (HOMO, HOMO − 1 to LUMO transition) may be explained using the results in Figure 3 together with Michl's perimeter model.[13] When aromatics such as acenaphthylene or benzene are added to the pyrrole rings of cyclo[10]pyrrole, whether the ring annulation results in a stabilization or a destabilization is related to the presence and absence, respectively, of nodal planes through the ten pyrrole N atoms and the peripheral fused aromatics. Thus, compared with a LUMO, which has bonding interaction with the annulated aromatics, the LUMO + 12 with ten nodal planes and having antibonding interaction with the annulated ring is greatly destabilized (Figure 4), resulting in an

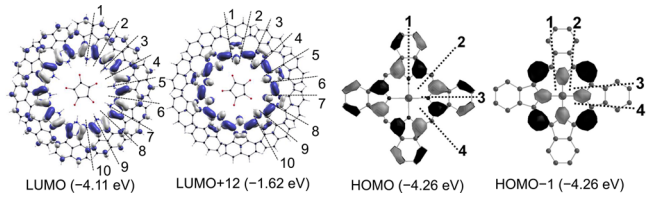

Figure 4. Nodal patterns of the LUMO and LUMO + 12 of **1b** (left) and the HOMO and HOMO − 1 of TBP (right) at an isosurface value of 0.025 atomic units (hartrees) with the $M_L = \pm 10$ and ±4 nodal plane properties highlighted.

increase in the (LUMO + 12 − LUMO) value (Figure 3), and a further decrease of the (HOMO − LUMO) value, i.e., a red-shift of the L band. Conversely, in the case of normal porphyrinoids such as tetrabenzoporphyrin (TBP), an antibonding interaction occurs for MOs having nodal planes through the four pyrrole N atoms (Figure 4), producing an increase in the (HOMO − HOMO − 1) value. As nicely explained by Gouterman's 4-orbital model,[14] the Q-band gains intensity, as the energy difference between the HOMO and HOMO − 1 increases. In a similar manner, a large energy difference between the LUMO + 12 and LUMO (Figure 3) produces the intensified L band in this study.

In summary, the acenaphthylene-fused cyclo[10]pyrrole complex **1b** has been synthesized selectively via an oxidative coupling reaction of the corresponding 2,2′-bipyrrole with croconate anion as a template. The structures of the largest isolated cyclo[10]pyrroles (**1a**,**1b**) were elucidated by X-ray crystallographic analysis. As a result of the absence of *meso*-atoms, as well as steric hindrance at the ligand periphery due to the large acenaphthylene moiety and many *tert*-butyl groups, the complexes adopt a markedly saddled structure. The electronic structure is also different from those of normal porphyrinoids, as follows. (1) The L band, which corresponds to the Q-band of normal porphyrins, shifted from ca. 500−550 nm to ca. 2000 nm and simultaneously intensified as a result of the fusion of the acenaphthylene molecules. (2) In contrast to normal porphyrins, which have doubly degenerate LUMOs, the HOMOs are doubly degenerate in cyclo[10]pyrroles, and this was conceptually explained by using a cyclic perimeter of $C_{30}H_{30}^{8-}$ hydrocarbon, experimentally proven by negative MCD $\mathcal{A}$-terms, and supported by MO calculations. (3) A strong absorption band was observed between the B and L bands, which was assigned to the CT band from the core of cyclo[10]pyrrole to the peripheral acenaphthylene moiety. However, similarly to previously reported porphyrinoids, both the electronic absorption and

DOI: 10.1021/jacs.6b04941
J. Am. Chem. Soc. 2016, 138, 7540−7543

MCD spectra can be readily assigned using Michl's perimeter model.

■ ASSOCIATED CONTENT

Supporting Information

The Supporting Information is available free of charge on the ACS Publications website at DOI: 10.1021/jacs.6b04941.

Experimental procedures, spectral data, and computational details (PDF)
Crystallographic summary (**1a**) (CIF)
Crystallographic summary (**1b**) (CIF)

■ AUTHOR INFORMATION

Corresponding Authors

*okujima.tetsuo.mu@ehime-u.ac.jp
*nagaok@shinshu-u.ac.jp

Notes

The authors declare no competing financial interest.

■ ACKNOWLEDGMENTS

This work was partially supported by JSPS KAKENHI 26410052 (TO), MEXT KAKENHI 25110003 (HU) and JSPS KAKENHI 15H00910, and JSPS (Japan)-NRF (South Africa) joint research program (NK). We thank Prof. Masanobu Uchiyama (University of Tokyo and RIKEN) and Dr. Atsuya Muranaka (RIKEN) for the near-IR MCD measurements, and the Advanced Research Support Center, Ehime University, for their assistance in obtaining the MALDI-TOF mass spectra. The X-ray diffraction studies were performed at the BL38B1 of SPring-8 with the approval of the Japan Synchrotron Radiation Research Institute (JASRI; proposal nos. 2013A1104, 2014B1168, 2015A1174).

■ REFERENCES

(1) (a) Seidel, D.; Lynch, V.; Sessler, J. L. *Angew. Chem., Int. Ed.* **2002**, *41*, 1422. (b) Sessler, J. L.; Karnas, E.; Kim, S. K.; Ou, Z.; Zhang, M.; Kadish, K. M.; Ohkubo, K.; Fukuzumi, S. *J. Am. Chem. Soc.* **2008**, *130*, 15256. (c) Eller, L. R.; Stępień, M.; Fowler, C. J.; Lee, J. T.; Sessler, J. L.; Moyer, B. A. *J. Am. Chem. Soc.* **2007**, *129*, 11020. (d) Stępień, M.; Donnio, B.; Sessler, J. L. *Angew. Chem., Int. Ed.* **2007**, *46*, 1431.

(2) (a) Okujima, T.; Jin, G.; Matsumoto, N.; Mack, J.; Mori, S.; Ohara, K.; Kuzuhara, D.; Ando, C.; Ono, N.; Yamada, H.; Uno, H.; Kobayashi, N. *Angew. Chem., Int. Ed.* **2011**, *50*, 5699. (b) Okujima, T.; Ando, C.; Mack, J.; Mori, S.; Hisaki, I.; Nakae, T.; Yamada, H.; Ohara, K.; Kobayashi, N.; Uno, H. *Chem. - Eur. J.* **2013**, *19*, 13970. (c) Okujima, T.; Ando, C.; Mori, S.; Nakae, T.; Yamada, H.; Uno, H. *Heterocycles* **2014**, *88*, 417.

(3) (a) Roznyatovskiy, V. V.; Lim, J. M.; Lynch, V. M.; Lee, B. S.; Kim, D.; Sessler, J. L. *Org. Lett.* **2011**, *13*, 5620. (b) Sarma, T.; Panda, P. K. *Chem. - Eur. J.* **2011**, *17*, 13987.

(4) Bui, T.-T.; Iordache, A.; Chen, Z.; Roznyatovskiy, V. V.; Saint-Aman, E.; Lim, J. M.; Lee, B. S.; Ghosh, S.; Moutet, J.-C.; Sessler, J. L.; Kim, D.; Bucher, C. *Chem. - Eur. J.* **2012**, *18*, 5853.

(5) Zhang, Z.; Cha, W.-Y.; Williams, N. J.; Rush, E. L.; Ishida, M.; Lynch, V. M.; Kim, D.; Sessler, J. L. *J. Am. Chem. Soc.* **2014**, *136*, 7591.

(6) The diffraction data were corrected for Lorentz, polarization, and absorption effects. The structures were solved with SIR2004 and refined with SHELXL-97. All calculations were performed by using the Crystal Structure crystallographic software package. CCDC-1049962 (**1a**) and CCDC-1049887 (**1b**) contain the supplementary crystallographic data for this paper. These data can be obtained free of charge from the Cambridge Crystallographic Data center via www.ccdc.cam.ac.uk/data_request/cif.

(7) SIR2004: an improved tool for crystal structure determination and refinement Burla, M. C.; Caliandro, R.; Camalli, M.; Carrozzini, B.; Cascarano, G. L.; De Caro, L.; Giacovazzo, C.; Polidori, G.; Spagna, R. *J. Appl. Crystallogr.* **2005**, *38*, 381.

(8) SHELXL-97: Program for solution and refinement of crystal structures from diffraction data, University of Göttingen, Göttingen, Germany; *"A short history of SHELX"*. Sheldrick, G. M. *Acta Crystallogr., Sect. A: Found. Crystallogr.* **2008**, *A64*, 112.

(9) Rigaku. *Crystal Structure*, version 3.8.2 or 4.0.1; Rigaku Corporation, Tokyo, Japan, 2010.

(10) Frisch, M. J.; Trucks, G. W.; Schlegel, H. B.; Scuseria, G. E.; Robb, M. A.; Cheeseman, J. R.; Scalmani, G.; Barone, V.; Mennucci, B.; Petersson, G. A.; Nakatsuji, H.; Caricato, M.; Li, X.; Hratchian, H. P.; Izmaylov, A. F.; Bloino, J.; Zheng, G.; Sonnenberg, J. L.; Hada, M.; Ehara, M.; Toyota, K.; Fukuda, R.; Hasegawa, J.; Ishida, M.; Nakajima, T.; Honda, Y.; Kitao, O.; Nakai, H.; Vreven, T.; Montgomery, J. A., Jr.; Peralta, J. E.; Ogliaro, F.; Bearpark, M.; Heyd, J. J.; Brothers, E.; Kudin, K. N.; Staroverov, V. N.; Kobayashi, R.; Normand, J.; Raghavachari, K.; Rendell, A.; Burant, J. C.; Iyengar, S. S.; Tomasi, J.; Cossi, M.; Rega, N.; Millam, J. M.; Klene, M.; Knox, J. E.; Cross, J. B.; Bakken, V.; Adamo, C.; Jaramillo, J.; Gomperts, R.; Stratmann, R. E.; Yazyev, O.; Austin, A. J.; Cammi, R.; Pomelli, C.; Ochterski, J. W.; Martin, R. L.; Morokuma, K.; Zakrzewski, V. G.; Voth, G. A.; Salvador, P.; Dannenberg, J. J.; Dapprich, S.; Daniels, A. D.; Ö., Farkas, Foresman, J. B.; Ortiz, J. V.; Cioslowski, J.; Fox, D. J. *Gaussian 09*, revision A.02; Gaussian, Inc.: Wallingford, CT, 2009.

(11) Köhler, T.; Seidel, D.; Lynch, V.; Arp, F. O.; Ou, Z.; Kadish, K. M.; Sessler, J. L. *J. Am. Chem. Soc.* **2003**, *125*, 6872.

(12) (a) Mack, J.; Stillman, M. J.; Kobayashi, N. J. *Coord. Chem. Rev.* **2007**, *251*, 429. (b) Kobayashi, N.; Muranaka, A.; Mack, J. In *Circular Dichroism and Magnetic Circular Dichroism Spectroscopy for Organic Chemists*; Royal Society of Chemistry: London, 2011.

(13) (a) Michl, J. *J. Am. Chem. Soc.* **1978**, *100*, 6801. (b) Michl, J. *Pure Appl. Chem.* **1980**, *52*, 1549. (c) Michl, J. *Tetrahedron* **1984**, *40*, 307.

(14) (a) Gouterman, M. *J. Chem. Phys.* **1959**, *30*, 1139−1161. (b) Fukuda, T.; Kobayashi, N. In *Handbook of Porphyrin Science*; Kadish, K. M., Smith, K. M., Guilard, R., Ed. World Scientific: Singapore, 2010; Vol. *9*.

DOI: 10.1021/jacs.6b04941
J. Am. Chem. Soc. 2016, 138, 7540−7543